



Investigation of the Effect of Anode Fuel Contaminants on the Performance of Polymer Electrolyte Membrane Fuel Cell

A. Moradi Bilondi¹, M. J. Kermani^{2*}, H. Heidary³, M. M. Abdollahzadeh⁴

^{1,2}Department of Mechanical Engineering, Amirkabir University of Technology (Tehran Polytechnic), Tehran, Iran

³ Faculty of Science, Qom University of Technology, Qom, Iran

⁴ Faculty of Mechanical of engineering, University of Guilan, Rasht, Iran

ABSTRACT: In the present work, a two-dimensional, transient, two-phase (two-fluid model), multicomponent model is considered for the anode-side of polymer electrolyte membrane fuel cells. The cell is assumed to include flow channel, gas diffusion layer, and catalyst layer. The discretized governing equations are numerically solved on a non-uniform grid with an in-house developed code. First, the steady-state effects of introducing Carbon-Monoxide-contaminated hydrogen on the cell performance were investigated. Then, the dynamic behavior of the cell under Carbon-Monoxide poisoning and the effects of air bleeding on the recovery of the output current density were investigated. The results were validated against experimental data, and it was indicated that even introducing a trace amount of contamination leads to significant degradation of cell performance (about 70% of output current was lost within 30 minutes when the hydrogen is pre-mixed with 10 part per million of Carbon Monoxide). Injecting a small amount of air into the anode stream resulted in a fast recovery of the lost current density (by injecting about 5% air into anode fuel, 80% of the output current was recovered within 2 minutes at 53 part per million Carbon Monoxide). Higher air bleeding ratio only resulted in minor improvement of the cell performance.

Review History:

Received: 07/11/2017

Revised: 19/01/2018

Accepted: 19/02/2018

Available Online: 25/02/2018

Keywords:

Polymer electrolyte membrane fuel cell

Two-phase flow

Numerical simulation

Carbon monoxide poisoning

Air bleeding

1. INTRODUCTION

The fuel cells have been considered as the main candidate of future clean power generation devices for stationary and transport applications. Due to the low operating temperature of Polymer Electrolyte Membrane (PEM) fuel cells and the technical and practical issues associated with the economic method of hydrogen production through steam reforming of hydrocarbon fuels, contamination of the hydrogen fuel stream by impurities (such as Carbon monoxide (CO)) is inevitable. The steady state and transient effects of CO poisoning on the fuel cell performance was investigated in several studies [1-3]. Springer et al. [1] developed the first pseudo two-dimensional steady state kinetic model for CO poisoning. Also, Chu et al. [2] presented a one-dimensional, transient model in order to investigate the CO poisoning effect over time based on the model developed by Springer et al. [1]. Furthermore, some mitigation methods, which one of these, is the oxygen bleeding was reported in several studies. Baschuk et al. [3] presented a one-dimensional steady state kinetic model to simulate the CO poisoning effects and the oxygen bleeding as one of the CO mitigation techniques.

In the present study, a comprehensive investigation

of the steady-state and transient effect of introducing the CO contaminant into the anode feed stream through a computational fluid dynamics analysis and the two-phase flow modeling is reported. Also, the effect of injecting air into the poisoned fuel (air bleeding) in order to mitigate the destructive effects of CO poisoning is studied.

2. DESCRIPTION OF THE MATHEMATICAL MODEL

In this section, the reaction kinetics and governing equations of the model used in the simulation are presented and discussed. The model is based on a single domain approach where all the governing equations are solved throughout the entire domain, without imposing the boundary conditions at the interfaces between different zones. The computational domain of anode-side in this study includes the gas channel, Gas Diffusion Layer (GDL), and the Catalyst Layer (CL). A set of conservation equations including mass, momentum, species, and liquid water equations, as well as, H₂, CO and O₂ coverage fraction equations are summarized as follows:

Mass conservation of the gas mixture [4]:

$$\frac{\partial(\rho_g \varepsilon (1-s))}{\partial t} + \nabla(\rho_g \bar{u}_g) = \sum_i S_i \quad (1)$$

*Corresponding author's email: mkermani@aut.ac.ir



Momentum conservation of the gas mixture [4]:

$$\frac{1}{\varepsilon(1-s)} \frac{\partial(\rho_g \bar{u}_g)}{\partial t} + \frac{1}{\varepsilon^2(1-s)^2} \nabla \cdot (\rho_g \bar{u}_g \bar{u}_g) = -\nabla p_g \quad (2)$$

$$+ \frac{1}{\varepsilon(1-s)} \nabla \cdot (\mu_g \nabla \bar{u}_g) - \frac{\mu_g}{KK_{rg}} \bar{u}_g$$

Species conservation of the gas mixture [4]:

$$\frac{\partial(\rho_g \varepsilon(1-s)X_i)}{\partial t} + \nabla \cdot (\rho_g \bar{u}_g X_i) = \nabla \cdot (\rho_g D_i^{eff} \nabla X_i) + S_i \quad (3)$$

$i = H_2, H_2O, CO, O_2$

Liquid water transport equation [4]:

$$\frac{\partial(\rho_l \varepsilon s)}{\partial t} + \nabla \cdot \left(\rho_l \frac{k_{rl} \mu_g}{k_{rg} \mu_l} \bar{u}_g \right) = -\nabla \cdot \left(\rho_l \frac{KK_{rl}}{\mu_l} \frac{dP_c}{ds} \nabla s \right) \quad (4)$$

$$+ S_{g-l} M_{h2o}$$

H_2 coverage fraction equation [3, 5, 6]:

$$\rho_{Pt} \frac{\partial \theta_H}{\partial t} = k_{fh} p_{H_2} (1 - \theta_{CO} - \theta_O - \theta_H)^n - b_{fh} k_{fh} \theta_H^n \quad (5)$$

$$- 2k_{eh} \theta_H \sinh\left(\frac{\alpha_a \eta F}{RT}\right) - k_{oh} \theta_H^n \theta_O$$

CO coverage fraction equation [3, 5, 6]:

$$\rho_{Pt} \frac{\partial \theta_{CO}}{\partial t} = k_{fc} p_{CO} (1 - \theta_{CO} - \theta_O - \theta_H) - b_{fc} k_{fc} \theta_{CO} \quad (6)$$

$$- k_{ec} \theta_{CO} \exp\left(\frac{\alpha_{CO} \eta F}{RT}\right) - k_{oc} \theta_O \theta_{CO}$$

O_2 coverage fraction equation [3, 5, 6]:

$$\rho_{Pt} \frac{\partial \theta_O}{\partial t} = k_{fo} p_{O_2} (1 - \theta_{CO} - \theta_O - \theta_H)^n \quad (7)$$

$$- b_{fo} k_{fo} (\theta_O)^n - k_{oh} \theta_H^n \theta_O - k_{oc} \theta_{CO} \theta_O$$

where u_g is the superficial velocity vector of gas mixture, ε porosity of the porous electrode, s the liquid water saturation, K the absolute permeability in the porous electrodes, K_{rg} and K_{rl} the relative permeability for the gas and liquid phase, X_i the mass fraction, D_i^{eff} the effective diffusion coefficient, and P_c is the capillary pressure. In the Eqs. (5) to (7), the parameter n represents the order of the reaction. Also, θ_i denotes the fraction of catalyst site occupied by species i , k the forward rate constant, and b is the backward-to-forward adsorption ratio. The last terms in Eqs. (1) and (3) are the volumetric sink or source terms due to the electrochemical reactions in the catalyst layer, and they are zero in other parts of the computational domain. Also, the last term in Eq. (4) is the mass transport rate of water due to the evaporation which is given in Refs. [3, 4, 6].

3. RESULTS AND DISCUSSION

Steady state CO poisoning effects

Fig. 1 presents the anode overpotential as a function of the current density for various concentrations of CO in the hydrogen gas streams. Results indicate that the anode overpotential increases with the increment of CO

concentration in the anode gas streams. As shown in Fig. 1, the predicted results are in good agreement with the experimental results of Lee et al. [7]. In the present steady-state simulation of CO poisoning, second order H_2 adsorption was considered (i.e., $n=2$). Table 1 gives the parameters used in this steady-state simulation. Other parameters were adopted from ref [7].

In these results, three distinct regimes are visible at high concentrations of CO (50 ppm and 100 ppm). In the low current density regime (until 0.2 A cm^{-2} for 50 ppm and until 0.1 A cm^{-2} for 100 ppm), a relatively small increase in the anode overpotential is observed and the cell performance is not affected by the poisoned catalyst site. When the output current density becomes greater than a limiting current density which is 0.3 A cm^{-2} for 50 ppm and 0.1 A cm^{-2} for 100 ppm, the increase in the anode overpotential is significant, indicating that the cell performance is strongly influenced by CO poisoning. This significant rise in the anode overpotential leads to a great acceleration in the CO electro-oxidation rate, which rapidly removes the CO from the catalyst surface [8]. When the current density further increases (more than 0.5 A cm^{-2} for 50 ppm and more than 0.3 A cm^{-2} for 100 ppm), the slope of the change is reduced and the anode overpotential increases with a slight gradient and the fuel cell voltage goes up to zero gently.

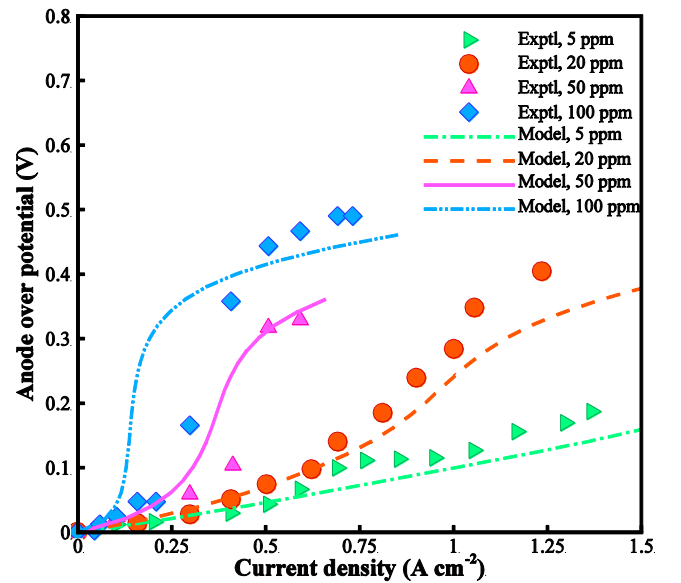


Fig. 1: Anode overpotential for the various concentration of CO in the anode gas stream [7]

Table 1. Parameters used for the analysis of CO poisoning

Parameter	Value[7]	Unit
b_{fc}, b_{fn}	4.5e-5 , 0.5	atm
k_{fc}, k_{fn}	0.06 , 3	$\text{A cm}^{-2} \text{ atm}^{-1}$
k_{ec}, k_{eh}	5e-9 , 0.75	A cm^{-2}
α_a	0.5 , -	-

Transient CO poisoning effects

The effect of CO concentration on the dynamic response of the cell current density is shown in Fig. 2. The values of cathode exchange current density and transfer coefficient are $i_{oc} = 1.2 \times 10^{-5}$ (A cm⁻²), $\alpha_a = 0.36$, $\alpha_c = 1$. The parameters used in the modeling are taken from Ref. [5]. In this simulation, first order H₂ adsorption was considered, i.e., $n=1$. When CO is introduced into the H₂ fuel stream, the current density decreases sharply (a drop in the current density from 1800 to 600 mA cm⁻² at 10 ppm), this dramatic drop shows that the presence of very low levels of CO has a significant detrimental effect on cell performance. After a long time, the current density eventually reaches a steady-state current density. By increasing the CO concentration, the time required to reach a steady state current density is decreased. For example, at 10 ppm, the steady state time is about 33 minutes, while at 100 ppm, this steady-state time is reduced to 17 minutes. CO concentration also affects the steady-state current density. As the CO concentration is increased, the steady-state current density decreases. For example, the steady-state current density decreases from 0.6 to 0.06 mA cm⁻² when the CO levels are increased from 10 to 100 ppm. Although an increase in the CO concentration decreases the steady-state current density, the amount of these changes decreases with increasing CO levels, so that the change in the steady state current density at 90 ppm to 100 ppm is very small. Therefore, the steady-state current density is more sensitive to changes in CO concentration at low levels of CO.

Effect of air bleeding

One of the ways to reduce the CO poisoning effects is to introduce the O₂ or air into the anode stream. Fig. 3 shows the variation of the current density at a voltage of 0.6 V over time. In this figure, a comparison between the experimental results [5] and the results of numerical modeling has been made. Although the simulation does not match the experimental data exactly for all cases, it does predict the general trend of transient poisoning and air bleeding and demonstrates the combined effects that air and CO can have on the cell performance. The cathode is fed with pure O₂ during the entire simulation. At $t = 1.5$ min, 53 ppm CO is introduced into the fuel, which leads to a reduction of the output current density (from 1800 to 150 mA cm⁻²) over 8.5 minutes. At $t = 27.5$ min, different levels of air (2%, 3%, 5%, 20% air)

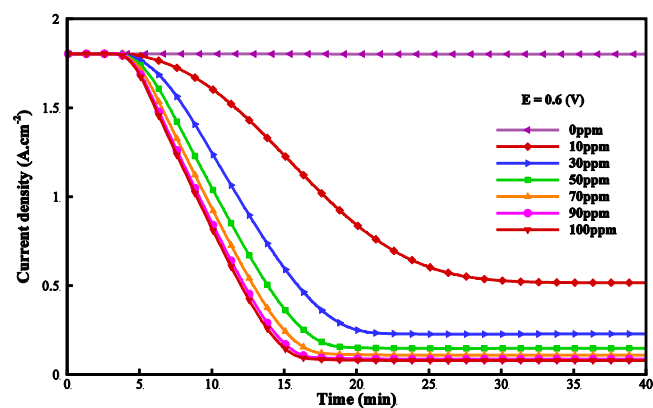


Fig. 2. Effect of CO concentration on cell performance

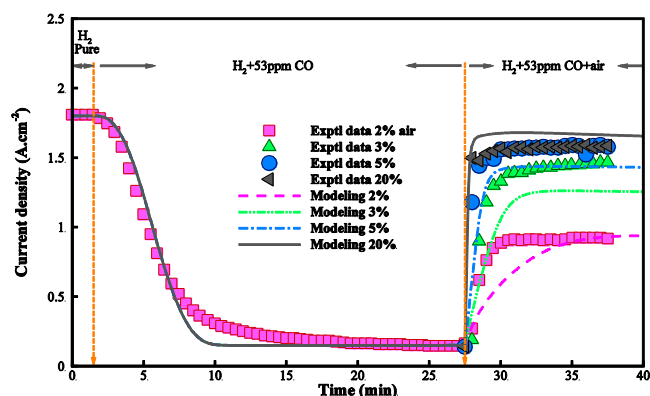


Fig. 3: Effect of anode air bleeding on the output current density [5]

were introduced into the CO-poisoned cell, and as the results indicate, the output current density is increased quickly afterward. The reason for this fast recovery is that oxygen molecules react and oxidizes the adsorbed CO molecules, which results in the mitigation of CO and production of CO₂. Removing CO from the surface catalyst leads to increasing the available surfaces for HOR reaction and then, more H₂ is oxidized, and eventually, the output current density is increased.

When 2% of air is injected into hydrogen fuel, the output current density rises rapidly from 150 to 937 mA cm⁻² (about 30% of the initial current density is recovered). When 3% of air is injected, the current density is increased to 1260 mA cm⁻² (about 68% of the initial current density is recovered), when 5% of air is injected, the current density is increased to 1435 mA cm⁻² (about 78% of the initial current density is recovered), and when 20% air is injected, the current density reaches to 1675 mA cm⁻² (about 92% of the initial current density is recovered).

In the low air bleeding region (0–3%), the current density is increased significantly and recovered as the air bleeding concentration is increased. In the high air bleeding region (>5%), only a minor improvement of output current density is seen as the air bleeding concentration is increased. This suggests that air bleeding at a low air concentration is more effective than that at a high air concentration. At a high air level, nitrogen may dilute the concentration of hydrogen and part of the hydrogen may also be oxidized by the oxygen in the air.

4. CONCLUSIONS

The main conclusions of this research are as follows:

1. The presence of a very low amount of carbon monoxide impurities in hydrogen fuel leads to a sharp drop in fuel cell performance.
2. When the CO concentration in the anode inlet feed increases, the sharp voltage drop (critical current density) begins at lower current densities.
3. The steady-state current density is more sensitive to changes in CO concentration at low levels of CO.
4. Injection a small amount of air into contaminated fuel results in a fast recovery of the lost current density.

REFERENCES

- [1] T. Springer, T. Rockward, T. Zawodzinski, S. Gottesfeld, Model for polymer electrolyte fuel cell operation on reformat feed: effects of CO, H₂ dilution, and high fuel utilization, *Journal of the Electrochemical Society*, 148(1) (2001) A11-A23.
- [2] H. Chu, C. Wang, W. Liao, W. Yan, Transient behavior of CO poisoning of the anode catalyst layer of a PEM fuel cell, *Journal of Power Sources*, 159(2) (2006) 1071-1077.
- [3] J. Baschuk, X. Li, Modelling CO poisoning and O₂ bleeding in a PEM fuel cell anode, *International Journal of Energy Research*, 27(12) (2003) 1095-1116.
- [4] X. Liu, G. Lou, Z. Wen, Three-dimensional two-phase flow model of proton exchange membrane fuel cell with parallel gas distributors, *Journal of Power Sources*, 195(9) (2010) 2764-2773.
- [5] L.-Y. Sung, B.-J. Hwang, K.-L. Hsueh, F.-H. Tsau, Effects of anode air bleeding on the performance of CO-poisoned proton-exchange membrane fuel cells, *Journal of Power Sources*, 195(6) (2010) 1630-1639.
- [6] N. Zamel, X. Li, Effect of contaminants on polymer electrolyte membrane fuel cells, *Progress in Energy and Combustion Science*, 37(3) (2011) 292-329.
- [7] S. Lee, S. Mukerjee, E. Ticianelli, J. McBreen, Electrocatalysis of CO tolerance in hydrogen oxidation reaction in PEM fuel cells, *Electrochimica Acta*, 44(19) (1999) 3283-3293.
- [8] H. Ju, K.-S. Lee, and S. Um, "Multi-dimensional modeling of CO poisoning effects on proton exchange membrane fuel cells (PEMFCs)," *J. Mech. Sci. Technol.*, vol. 22, no. 5, pp. 991-998, 2008.